Eco-evolutionary dynamics lead to functionally robust and redundant communities

Lorenzo Fant,[1,*] Iuri Macocco,[1,*] and Jacopo Grilli[2,†]

[1] *International School for Advanced Studies (SISSA), Via Bonomea 265, 34136 Trieste, Italy*

[2] *The Abdus Salam International Centre for Theoretical Physics (ICTP), Strada Costiera 11, 34014 Trieste, Italy*

Microbial communities are functionally stable and taxonomically variable. Species abundance greatly fluctuates over time and across communities. The functional composition, measured with the gene content of metagenomic data, is instead robust and conserved over time and across similar environments. These observations together suggest that species are functionally redundant: the same function is performed by many species, and one can assemble many communities with different species and the same functional composition. The clarity of this observation does not parallel with a theoretical understanding of its origin. Here we study a broad class of consumer-resource models with cross-feeding under an eco-evolutionary framework, in presence of a metabolic tradeoff. We show that the eco-evolutionary trajectories separate in a fast and a slow dynamics. The fast dynamics are determined by niche differences and make the system converge to a set of solutions uniquely determined by resource input, which we identify analytically. The slow dynamics occur entirely within that set of solutions and are determined by the interplay between fitness differences and niche differences. Interestingly, the set of solutions determined by the fast eco-evolutionary dynamics uniquely corresponds to the functional composition of the community, characterized by the fraction of individuals able to perform a given function, and not by the species content. We finally show then that a small variation of the fitness differences determines only a variation of the species composition, leaving the functional profile unvaried.

Main

The staggering taxonomic diversity of microbial communities parallels with their remarkable functional robustness [1, 2]. At the species and strain level, their taxonomic composition is in fact highly variable across communities with similar environmental conditions and over time. This variability is also observed in microcosmos experiments, under very controlled conditions [3]. On the other hand, the functional composition of communities, estimated for instance using metagenomic data [2, 4], appears highly reproducible and stable over time. This — only apparent — contradiction strongly suggests that microbial taxa are highly functional redundant: since many species can perform the same functions, there exist multiple species combinations corresponding to the same functional profile.

While this observation is robust and replicated across ecosystems, including — at least some — laboratory experiments, its origin is unknown. This lack of understanding is, in part, due to the fact that the vast majority of the modelling frameworks focus on species composition. Population abundances are in fact the standard degrees of freedom of mathematical models of community dynamics.

Consumer-resource models are the main modelling framework for microbial communities. Their origin goes back to the classic work of MacArthur and Levins [5], which has been extensively studied and discussed in the following decades [6, 7], mostly to describe the coexistence of a handful of species.

---

*These two authors contributed equally

†Electronic address: `jgrilli@ictp.it`

Recently, they have been furtherly extendend to consider facilitation through cross-feeding [3, 8, 9], where species change resource availability not only by consumption, but also because they release in the environment the waste products of their metabolism. Such improvements effectively describe experimental results [3] and have the flexibility to reproduce patterns observed in empirical microbial communities [10].

Once the parameters of the model are set and an initial pool of species is chosen, populations converge for large times to an equilibrium point. Under some mild conditions, identified over decades of theoretical work [11, 12], consumer-resource models are characterized by a globally stable equilibrium: the steady state is independent of the initial population abundances and resource concentrations. The competitive exclusion principle — one of the most fundamental results of theoretical ecology — limits the number of species that can possibly coexists in a stable equilibrium: diversity cannot exceed the number of resources. While this bound is hard, it is often not realized, as only fewer species are able to coexist.

The number and identity of the species coexisting at equilibrium is in fact determined not only by the ecological dynamics, but also by the initial pool of species. This pool of species is often interpreted as the metacommunity diversity: the ecological dynamics unfolds in a local community linked to the metacommunity by a small migration rate. Most of the recent progresses in understanding the assembly of large ecological communities have been driven by the assumption of "random" species pools [13–15]. This common choice implicitly assumes a separation of spatial and temporal scales: the ecological dynamics determining the community composition in the local community occurs independently of the evolutionary processes determining the pool of diversity of the metacommunity.

Instead of assuming an externally fixed species pool, one can let it evolve dynamically. Classic work in adaptive dynamics [16] has shown how, starting from a clonal population, diversification can evolve under general conditions on frequency dependent selection. Several works have then studied eco-evolutionary dynamics of interacting populations [17, 18], by allowing their parameters to be subject to mutations and be inherited by the following generation. Dynamic adaptation of metabolic preferences allows many species to coexist and respond optimally to environmental change [19]. A critical aspect of these models is the variation of parameters correspondig to fitness and niche differences, both contributing to the community evolution [20]. A key question is how the interplay between niche and fitness difference determine the species and functional composition of communities.

Here we consider the broad framework of consumer-resource-crossfeeding models under an explicit eco-evolutionary dynamics, where strains differ in their resource preference and in their intrinsic fitness. Higher resource intakes are balanced by a lower efficiency (or equivalently, higher mortality) implemented by a metabolic trade-off [21, 22]. We show that, when fitness differences are small, the evolutionary dynamics converges rapidly to a stationary and reproducible functional composition — here defined as the fraction of individuals able to grow on a given resource — which we analytically predict. Interestingly, we show that, once the functional attractor is reached, the strain dynamics is then dominated by fitness differences, implying that functional composition is robust (independent of small fitness differences) and redundant (is obtained under multiple strain compositions).

Eco-evolutionary dynamics

In our framework, individuals are characterized by a resource preference vector which determines the intake rate of each of the R resources available in the environment (relative to a maximum). An individual with preference $a_i = 0$

will not consume resource i, while an individual with preference $a_i = 1$ will consume it with the maximum intake rate ν_i. Consumed resources are converted into biomass with finite efficiency (equivalent to an inverse yield). We assume that the yield (or equivalently the death rate, see Materials and Methods) depends linearly on the number of resources consumed: the more resources an individual can grow on, the less efficiently it grows. Individuals also differ in their intrinsic fitness, modelled as an additional — strain dependent — term in the efficiency (or equivalently mortality).

Resource dynamics is described explicitly. Resources are introduced in the system with a resource-specific rate h_i and consumed by individuals. Their concentration also vary because of cross-feeding. A fraction $1 - \ell$ of resources consumed by an individual is used for growth, while a fraction ℓ is transformed to different resources and released again in the environment [8]. The cross-feeding matrix, with elements D_{ij}, specifies the relative rates of resource transformation (see Materials and Methods for its parameterization).

In our model, resource preferences are subject to mutations and evolution. After reproduction, the new individual can differ from the parent in its resource consumption. We consider different implementation of mutations (see Materials and Methods) which, however, do not affect the results. We restrict the analysis to the most conservative case of rare mutation, where offspring differs in the resource preference vector for at most one resource.

Mutated individuals also differ from parents in their intrinsic fitness, which is drawn at random independently of the parent fitness (see Materials and Methods). We restrict our analysis to the case of "small" fitness differences, where their magnitude is smaller than the typical effect of mutations in the resource preference in absence of competition (see Materials and Methods).

The per-capita growth rate of a strain μ — where with "strain" we identify the group of individuals with equal resource preference a_i — will therefore be a function $g_\mu(\underline{c})$ of the resource concentration $\underline{c}$, which, in turn, depends dynamically on the population abundance because of consumption and cross-feeding (see Materials and Methods). We consider the following choice

$$g_\mu(\underline{c}) = \eta_\mu \left(\sum_{i=1}^{R} a_{\mu i} r_i(c_i) - \delta \left(1 + \chi \sum_{i=1}^{R} a_{\mu i} \right) (1 + \epsilon_\mu) \right) \ . \tag{1}$$

The values of η_μ and δ are arbitrary and their choice does not affect the results. The functional form $r_i(c_i)$ encodes the functional response. Both linear and saturating (Monod-like) functional responses produce the same results. The parameter χ quantifies the fitness cost of consuming one resource and implements the metabolic trade-off. The form of the trade-off generalizes the case considered in [21, 22], which corresponds to the limit $\chi \to \infty$. The intrinsic fitness differences are determined by the value of ϵ_μ.

Convergence to the functional attractor

Fig 1 shows the resulting eco-evolutionary trajectories. Starting from a clonal population, a diverse community is rapidly assembled. Strain abundances changes abruptly following successful invasion events and keep changing over the whole duration of the simulations (over 10^5 invasion attempts).

The final community structure is remarkably simple if, instead of concentrating on its species abundances, we focus on its functional composition (see Materials and Methods). We define functional occurrence F_i as the fraction of individuals able to grow on i (i.e., with $a_i = 1$). After a short transient (of about 10^2 invasion attempts) the

functional occurrences and with the total biomass N relax to the respective stationary values F_i^* and N^* which are finely reproducible across different realizations.

Two phases characterize therefore the eco-evolutionary dynamics. The first phase is an initial-condition dependent transient, where the community structure is mainly shaped by rapid invasions. In the second phase, conversely, the community has converged to a stable functional composition, which we will refer to as "functional attractor".

The eco-evolutionary dynamics of the second phase unfolds while keeping the total biomass constant, affecting therefore the relative abundance of strains. The sequence of invasions and extinctions of strains is determined by the interplay of fitness differences ϵ_μ and niche differences, related to the dissimilarity of the resource preferences. Importantly, the trajectories of species abundances are effectively restrained to occur on the low(er)-dimensional manifold determined by the constraint enforced through the functional occurrences F_i^*. In this second phase the community has thus reached a "functional maturity" and the subsequent evolution only affects strain composition while leaving unaltered the functional one.

Ecological dynamics under infinite species pool predicts the functional attractor

The stability and reproducibility of the functional attractor suggest that it is possible to predict its properties. We considered a simplified setting which aims at mimicking the effective exploration of the phenotipic space performed by mutations. In particular we looked at the same ecological dynamics defined above but with an initial infinitely large species pool, which encompasses all the possible strains (i.e., the 2^R possible resource preferences). A similar approach has been considered to study a simpler version of the model [21] (corresponding to the limit $\chi \to \infty$ and no crossfeeding). We further postulate that the small istrinsic fitness differences do not affect substantially the functional attractor.

The consumer-resource-crossfeeding model with infinite species pool and no intrinsic fitness differences can be analytically solved by further assuming that the timescales of species and resource dynamics are separated. In the Materials and Methods we show that the stationary functional occurrences F_i^* and N^* are given by

$$F_i^* = \min\{\frac{h_i^{eff}}{\chi}\frac{1}{N^*}, 1\} \tag{2}$$

and

$$N^* = \frac{\sum_i h_i^{eff}}{R(1+\chi\sum_i F_i^*)} \ . \tag{3}$$

The parameter h_i^{eff} is the effective resource inflow in the system, which is given by the combination of resources that are externally supplied and the ones produced via crossfeeding. This quantity is in a simple linear relation to the inflow rate of externally provided resource h_i trough the crossfeeding matrix D (see Materials and Methods).

Figure 1 shows that the predictions of eq. 2 and eq. 3 accurately describe the outcomes of the eco-evolutionary dynamics. Resources can be partitioned in two groups based on their effective influx rate h_i^{eff}. If the influx rate is larger than a critical value h_c, then the ability to metabolize that resource is a "core" function, shared by each individual in the community (i.e., $F_i^* = 1$). The value of h_c depends on both the spread of resource quality (the variability among the h_i) and the metabolic cost χ. The higher the metabolic cost and the variability, the higher the critical quality threshold h_c and, consequently, the fewer the core resources.

Not all the individuals consume resources with quality lower than the critical threshold. A linear relation links the functional occurrence F_i^* with the resource quality h_i^{eff}. The slope of this relation is simply linked to the metabolic cost and the total biomass, being equal to $(\chi N^*)^{-1}$ (see Materials and Methods). Figure 1B shows that the analytical expression for N^* (as a function of the metabolic cost χ) is correctly matched by numerical simulations.

Functional stability and robustness

These results connecting resource quality with functional profile and total biomass can be generalized to a wider range of assumptions. For instance, one can go beyond dichotomous resources preferences, and consider species able to consume resources at different rates. As long as the species pool is large and variable enough, the results presented previously still hold. One can also include intrinsic differences between resources. For instance, some resources could have higher energy content or the maximal intake rate could be resource-dependent. These differences between resources can be easily reabsorbed in the quality parameters h_i^{eff} (see Materials and Methods).

An emerging feature of the present framework is that the functional composition of communities is extremely robust to fitness differences. We further explored this robustness by considering fitness variation across space and time. Figure 3 shows how species composition and functional profile change across communities or over time as species fitness differences change. Species composition varies widely: the small fluctuations in relative fitness determine which species go extinct and the relative abundance of those who survive. The functional composition is instead extremely robust to these fitness differences, closely reproducing the phenomenology observed in microbial communities [2].

Conclusion

Our results shed light on the composition of large ecological communities. When the species pool is not a-priori constrained, but is allowed to evolve, the complex ecological dynamics can be decomposed in a fast, predictable, component and a slow one, contingent to the (small, yet relevant) fitness differences. The community composition rapidly converges to a manifold of solution, determined by resource availability (see Figure 3). The dynamics on that manifold is governed by difference in relative fitness. Remarkably, this separation of fast and slow components maps directly into functional and taxonomical composition: the former is robust and governed only by resource quality, the latter is constrained by function, but free to move along functionally equivalent directions.

The functional reproducibility of communities is also affected by fitness differences. We have shown that a typical fitness difference of 1% does not alter substantially the functional composition. On the other hand, much smaller fitness differences substantially skew the taxonomic composition. The fitness differences, responsible for taxonomic variation over space and time, could by due by multiple factors (from abiotic factors to phages). Our framework provide a baseline to assess the role of this variation, and could be extended to include explicitly those factors contributing to fitness differences.

Here we assumed that intrinsic fitness was not heritable, and it was drawn from a constant distribution for every new mutant. The alternative choice [20], with heritable fitness differences, would likely produce the same results, provided that intrinsic fitness differences were not evolving rapidly. In this scenario, we expect again that the eco-evolutionary dynamics is divided in two phases. In the first, the community to converge to the functional attractor. In the second,

the strains keep evolving and the intrinsic fitnesses keep increasing, with the constraint imposed by the functional composition.

A remarkable aspect of our framework is that functional composition — as opposed to taxonomic composition — naturally emerges as the relevant, reproducible observable to characterize an ecological community evolved in a constant environment. This property is likely to hold more generally and not to be restricted to consumer-resource systems or microbial communities. We expect that a similar approach could be developed to study mutualistic communities or pathogen dynamics.

Materials and Methods

Definition of the model

We consider a consumer-resource model in presence of crossfeeding [8], which describes the dynamics of population biomasses n_σ (for $\sigma \in \mathcal{S}$) and resources concentration c_i (for $i \in R$). Changes in population abundance are defined by

$$\frac{dn_\sigma}{dt} = n_\sigma \left(\eta_\sigma \sum_{i \in R} \mathcal{E}^g_{i\sigma} - \delta_\sigma \right) \ . \tag{4}$$

where δ_σ is a death term and η_σ is the efficiency of the conversion of energy into biomass. $\mathcal{E}^g_{i\sigma}$ is the energy flux used for species σ to grow from metabolite i. The total energy flux into a cell of type σ is given by $\mathcal{E}^{in}_{i\sigma} = \mathcal{E}^g_{i\sigma} + \mathcal{E}^{out}_{i\sigma}$, where $\mathcal{E}^{out}_{i\sigma}$ are the energy fluxed of secreted metabolites. The associated dynamics of resource concentration c_i is defined by

$$\frac{dc_i}{dt} = h_i(c_i) - \frac{1}{w_i} \sum_{\sigma \in \mathcal{S}} n_\sigma \mathcal{E}^{in}_{i\sigma} + \frac{1}{w_i} \sum_{\sigma \in \mathcal{S}} n_\sigma \mathcal{E}^{out}_{i\sigma} \ , \tag{5}$$

were w_i defines the conversion between energy and concentration of resource i. The function $h_i(c_i)$ specify the dynamics of resource concentration in absence of consumers.

We assume that the energy fluxes used for growth are a constant fraction $1 - \ell$ of the total ones: $\mathcal{E}^g_{i\sigma} = (1 - \ell)\mathcal{E}^{in}_{i\sigma}$. The energy fluxed from secreted metabolites is given by $\mathcal{E}^{out}_{i\sigma} = \ell \sum_{j \in R} D_{ij} \mathcal{E}^{in}_{j\sigma}$. The crossfeeding matrix element D_{ij} defines energy conversion between resource j and resource i. Energy conservation implies $\sum_i D_{ij} = 1$.

The energy flux $\mathcal{E}^{in}_{i\sigma}$ is takes the form

$$\mathcal{E}^{in}_{i\sigma} = w_i \nu_i a_{\sigma i} r_i(c_i) \ , \tag{6}$$

where $r_i(c_i)$ is a non-decreasing function of the concentration of resource i, and ν_i is the maximal intake rate of resource i. The elements $a_{\sigma i} \in [0, 1]$ measures the intake rate of metabolite i species σ relative to the maximum ν_i. Here we focus on the case of externally supplied resources $h_i(c_i) = h_i$.

For the death rates and yield we assume the expression

$$\frac{\delta_\sigma}{\eta_\sigma} = \frac{1}{\tau} \left(1 + \chi \sum_{j \in R} a_{\sigma j} \right) \ . \tag{7}$$

Without loss of generality we can set the timescale $\tau = 1$. In the simple setting of $a_{\sigma j} \in \{0, 1\}$, the parameter χ measure the cost of being able to metabolize aech metabolite (χR is the fitness cost paid to be a generalist).

Metabolic tradeoffs and functional attractor

If the dynamics of resources is much faster than population dynamics, one can effectively describe the dynamics of populations as

$$\frac{dn_\sigma}{dt} = n_\sigma \left(\eta_\sigma \sum_{i \in R} a_{\sigma i} \nu_i \frac{h_i^{eff}}{\sum_{\mu \in \mathcal{S}} n_\mu a_{\mu i} \nu_i} - \delta_\sigma \right) \ , \tag{8}$$

where $h_i^{eff} = (1-\ell) \sum_{j \in R} B_{ij} h_j w_j$ and the matrix $B = (I - \ell D)^{-1}$. It is known [21] that

$$L(\{n\}) = \sum_\sigma \frac{\delta_\sigma}{\eta_\sigma} n_\sigma - \sum_i h_i^{eff} \log \left(\sum_\sigma \nu_i a_{\sigma i} n_\sigma \right) \ , \tag{9}$$

is a Lyapunov function. With our choice for the metabolic tradeoff (7), it can also be written as

$$L(\{n\}) = \sum_\sigma n_\alpha \left(1 + \chi \sum_{j \in R} a_{\sigma j} \right) - \sum_i h_i \log \left(\sum_\beta \nu_i a_{\beta i} n_\beta \right) \tag{10}$$

We then introduce the total population size $N = \sum_{\sigma \in \mathcal{S}} n_\sigma$ and define the functional abundances F_i as

$$F_i = \sum_{\sigma \in \mathcal{S}} a_{\sigma i} \frac{n_\sigma}{N} \ , \tag{11}$$

which corresponds to the fraction of individuals that are able to metabolize metabolite i. Interestingly, and surprisingly, the Lyapunov function can then be rewritten as function of N and $\{F\}$ alone:

$$L(N, \{F\}) = N \left(1 + \chi \sum_{j \in R} F_j \right) - \sum_{j \in R} h_j \log \left(N \nu_j F_j \right) \ . \tag{12}$$

By minimizing the function over F_i in $[0,1]$ we obtain

$$F_i^* = \min\{1, \frac{1}{N^*} \frac{h_i}{\chi}\} \ , \tag{13}$$

where the total biomass is the solution of

$$N^* = \frac{\sum_{j \in R} h_j}{\left(1 + \chi \sum_{j \in R} F_j^* \right)} \ . \tag{14}$$

We can now notice that the equilibrium solutions is primarily identified by its belonging to a manifold described by equations (13,14). For a given system, ordering the resources based on their h_i we can identify a set "core" resources. These are the most abundant ones that must to be metabolised in order to survive ($F_i = 1$).

This simpler prescription with time-scale separation between populations and resources allows us to analytically derive the properties of the stability manifold. Nonetheless, even if we were not able to find a close general expression for the Lyapunov in presence of resources dynamics and cross feeding, the computational results behave according to the same modelling developed in the simpler case.

A. Eco-Evolutionary dynamics

We assume a separation of timescales between the evolutionary and the ecological dynamics: once a mutant appears in the system, the ecological dynamics relaxes to its equilibirum before a new mutant appears.

We further assume that mutations are small. A mutant differ from the parent for the resource preference for only one resource. In the following, with a small abuse of notation, we will use the term "genome" to indicate the array of resource preference $a_{\sigma i}$ for strain σ, "locus" i to indicate a position in the genome (corresponding to the consumption of resource i), and "allele" to indicate whether a resource i is consumed or not ($a_{\sigma i} = 1$ or 0).

The mutation probability of each locus depends on the allele in that locus. The rate at which an allele 1 mutate to become 0 (deletion) is constant, independent of the locus, and equal to 1. The rate at which an allele 0 mutate to become 1 (addition) equals to $P_h F_i + P_{dn}$. The quantity P_h is the probability that an addition happens because of horizontal transfer, while P_{dn} the rate of "de novo" mutations. The rate of horizontal transfer is proportional to the frequency of the allele in the population F_i. Note that these choices make the mutation rate genome dependent: the probability that genome μ mutates equals

$$p_\mu = x_\mu \left(\sum_{i|a_{\mu i}=0} U_{+,i} + \sum_{i|a_{\mu i}\neq 0} U_{-,i} \right) \tag{15}$$

where x_μ is the frequency of genome μ in the population.

Since the mutant $\tilde{\mu}$ appears at a small frequency in the population, its survival probability of the new species is given by

$$p_{\tilde{\mu}}^{surv} = 1 - \min\left(1, \frac{(1+\chi\sum_i a_{\tilde{\mu}i})(1+\epsilon\delta)}{(1-l)\sum_i a_{\tilde{\mu}i} r_i(c_i)}\right) \tag{16}$$

Calculating all these quatities for all possible mutations of all existing genomes one can create a set of rates at which species μ mutates gene i

$$\underline{P}^{inv} = \left\{ p_\mu p_{i|\mu} P_{\tilde{\mu}}^{surv} \right\}_{i,\mu} \tag{17}$$

We eventually select a random mutation using $\underline{P}^{inv}$ as probabilities and considering $T = \frac{1}{\sum_{i\mu} \underline{P}^{inv}}$ as the mean time necessary for the evolution to take place.

Numerical Simulations

Numerical simulations were performed on an average desktop, using a custom Python package (available upon request). The integration of the coupled differential equations (4) and (5) was achieved with the standard solve_ivp function from the SciPy.integrate package. In particular we set a flag to stop the integration once $|\max_\sigma g_\sigma(\underline{c})| < 10^{-4}$, i.e. the populations are no more changing significantly. In the case of assembly, at each iteration a new patch is created from the previous one by dropping the taxa with relative abundance lower than a threshold (10^{-5}) and introducing a new strain with abundance equal to the threshold value itself. the system undergoes a fast initial transient and reaches the functional manifold within the very few first integration time steps; it then slowly evolves to the final equilibrium state. The latter is ensured to satisfy the stability creterium defined above. On the other hand, in presence of a time dependent noise all phenotypes were kept "available", since even a small change in the noise can make a phenotype enter the pool of relevant species.

Choice of parameters

The results presented in this paper were achieved using generic parameters, whose details can affect the distribution of taxa or relaxation time but not the macroscopic observables that characterise the stability manifold. Referring to eq. 4 and 5, for simplicity we selected $\eta_\sigma = \nu_i = w_i = 1$. The time scale τ was also set to 1. For the fitness difference, we used a gaussian noise of amplitude $\epsilon = 0.005$. A larger values of noise (of the order 0.1) often disrupts the properties of the manifold. For instance species not consuming a core resources is still able to survive because of a low death rate. On the other hand, for $\epsilon < 0.001$ the simulation became very long as the small fitness difference means a very slow decay of the less fit species. The cross-feeding matrix D has been chosen following [10]. Entries were extracted according to a Dirichlet distribution, where resources have been dividend in three classes. We chose an effective spersity of $s = 0.1$. The fraction of resources remaining in the same class was $f_s = 0.7$ while the ones going to the waste class is $f_w = 0.28$. The results of the simulations are independent of the choices of P_h and P_{dn}, which we considered equal to $P_h = 0.9$ and $P_{dn} = 0.1$

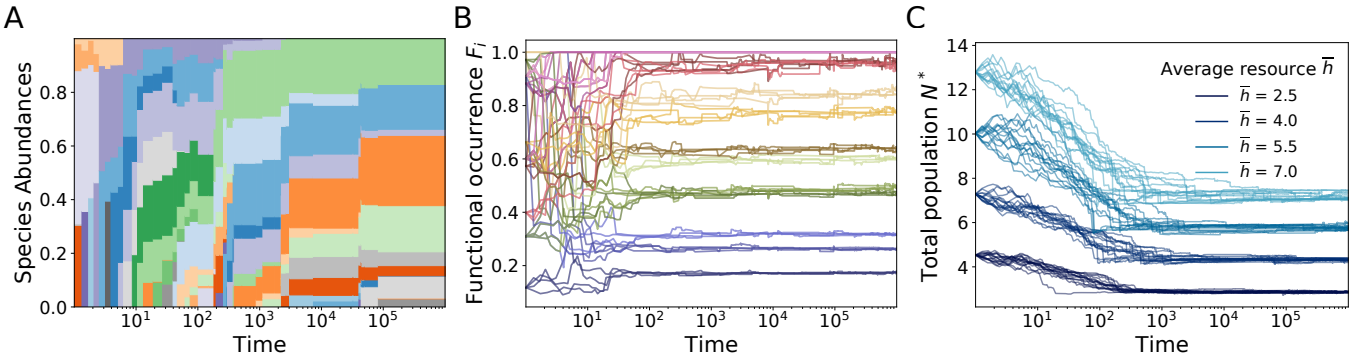

FIG. 1: Communities evolving under a consumer-resource model. the system is initialized with a low number of initial random species. The former are chosen so that each gene is present at least once. The system evolves in a chemostat with a fixed resources input. When equilibrium is reached, one mutant is added is added to the batch. The chemostat then equilibrates to a new fixed point and the procedure is repeated until function and biomass reach stability. **A**: Time evolution of the species relative abundances for one realisation of the system. **B**: Time evolution of functional occurrences for three different realisations of the system. 15 resource are given. **C**: Time evolution of the total biomass of the system. 20 realisations of the system are shown for each value of average resources income.

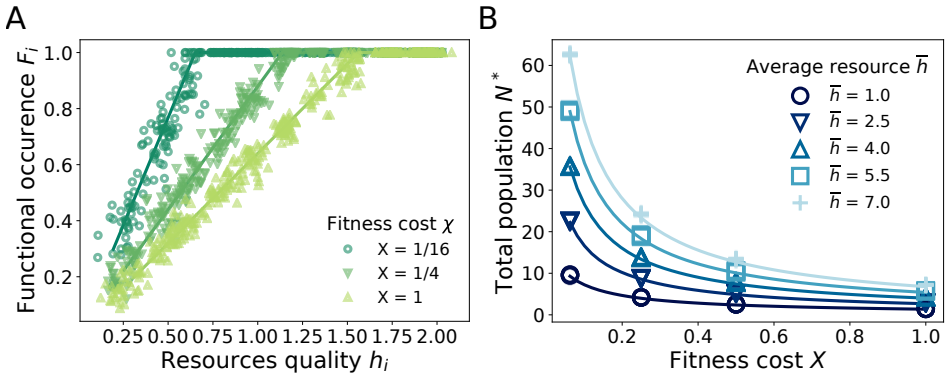

FIG. 2: The theoretical predictions given by eq. 13, 14 (solid lines) are reproduced by numerical integration of eq. 4, 5 (markers). **A**: Occurrence of the phenotypes F_i as a function of the resource income rates h_i. According to equation 13 the most abundant resources (core) are consumed by all species (F_i=1) while the remaining ones only by a fraction $F_i = \frac{h_i}{N^* \chi}$. Notice that increasing χ reflects in a decrease of the number of core resources. **C**: Dependence of the total equilibrium population N^* (biomass) on the value of χ. Unlike the the quantities in **A** here we here find a dependence on average value of the resources incomes $\overline{h}$. In each figure are represented 20 different noise realizations solutions of the system for each χ (**A** and each $\overline{h}$ (**B**)

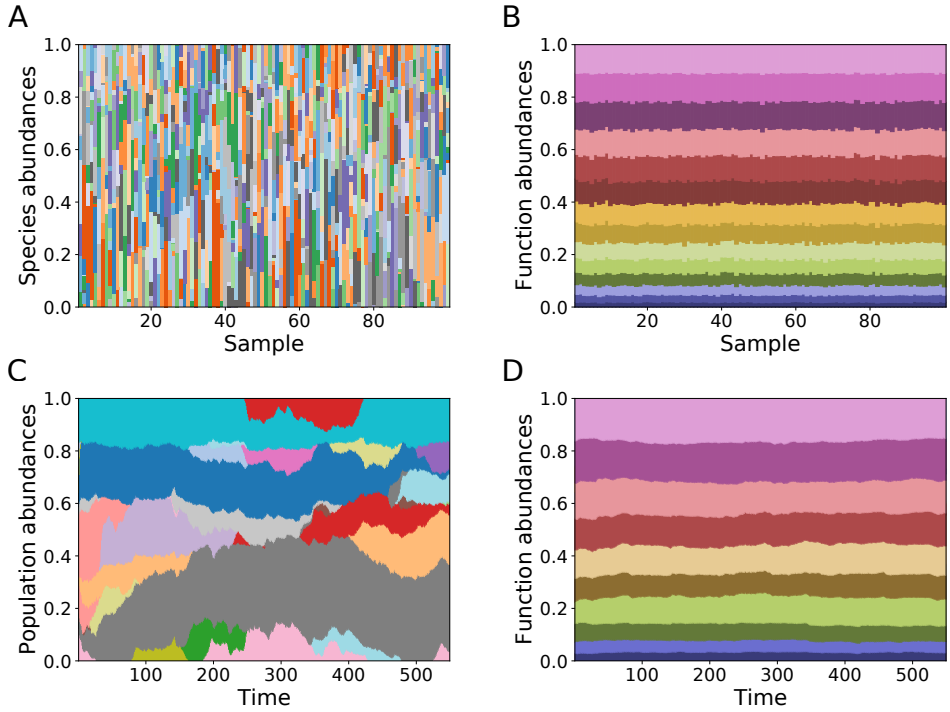

FIG. 3: Fitness differences allow to demonstrate how functional stability is already encoded within the model. While the populations/taxonomies becomes highly variable and heterogeneous, the functional composition is preserved and unaffected by stochasticity. **A**,**B** show a collection of equilibrium configurations of systems with different realisations of a static noise. **C**,**D** show the evolution of the composition of a system with a dynamically varying noise .

[1] Burke, C., Steinberg, P., Rusch, D., Kjelleberg, S. & Thomas, T. Bacterial community assembly based on functional genes rather than species. *Proceedings of the National Academy of Sciences* **108**, 14288–14293 (2011).

[2] Louca, S. *et al.* Function and functional redundancy in microbial systems (2018).

[3] Goldford, J. E. *et al.* Emergent simplicity in microbial community assembly. *Science* **361**, 469–474 (2018).

[4] Louca, S., Parfrey, L. W. & Doebeli, M. Decoupling function and taxonomy in the global ocean microbiome. *Science* **353**, 1272–1277 (2016).

[5] Macarthur, R. & Levins, R. The Limiting Similarity, Convergence, and Divergence of Coexisting Species. *The American Naturalist* **101**, 377–385 (1967).

[6] Tilman, D. A consumer-resource approach to community structure. *American Zoologist* **26**, 5–22 (1986).

[7] Chesson, P. Macarthur's consumer-resource model. *Theoretical Population Biology* **37**, 26–38 (1990).

[8] Marsland, R. *et al.* Available energy fluxes drive a transition in the diversity, stability, and functional structure of microbial communities. *PLoS Computational Biology* **15** (2019). 1805.12516.

[9] Butler, S. & ODwyer, J. P. Stability criteria for complex microbial communities. *Nature communications* **9**, 1–10 (2018).

[10] Marsland, R., Cui, W., Goldford, J. & Mehta, P. The community simulator: A python package for microbial ecology. *Plos one* **15**, e0230430 (2020).

[11] Case, T. J. & Casten, R. G. Global stability and multiple domains of attraction in ecological systems. *The American Naturalist* **113**, 705–714 (1979).

[12] Harrison, G. W. Global stability of predator-prey interactions. *Journal of Mathematical Biology* **8**, 159–171 (1979).

[13] Bunin, G. Ecological communities with lotka-volterra dynamics. *Physical Review E* **95**, 042414 (2017).

[14] Advani, M., Bunin, G. & Mehta, P. Statistical physics of community ecology: a cavity solution to macarthurs consumer resource model. *Journal of Statistical Mechanics: Theory and Experiment* **2018**, 033406 (2018).

[15] Cui, W., Marsland III, R. & Mehta, P. Effect of resource dynamics on species packing in diverse ecosystems. *Physical Review Letters* **125**, 048101 (2020).

[16] Geritz, S. A., Mesze, G., Metz, J. A. *et al.* Evolutionarily singular strategies and the adaptive growth and branching of the evolutionary tree. *Evolutionary ecology* **12**, 35–57 (1998).

[17] Ackland, G. & Gallagher, I. Stabilization of large generalized lotka-volterra foodwebs by evolutionary feedback. *Physical review letters* **93**, 158701 (2004).

[18] DeLong, J. P. & Gibert, J. P. Gillespie eco-evolutionary models (gem s) reveal the role of heritable trait variation in eco-evolutionary dynamics. *Ecology and evolution* **6**, 935–945 (2016).

[19] Pacciani-Mori, L., Giometto, A., Suweis, S. & Maritan, A. Dynamic metabolic adaptation can promote species coexistence in competitive communities. *PLoS computational biology* **16**, e1007896 (2020).

[20] Good, B. H., Martis, S. & Hallatschek, O. Adaptation limits ecological diversification and promotes ecological tinkering during the competition for substitutable resources. *Proceedings of the National Academy of Sciences* **115**, E10407–E10416 (2018).

[21] Tikhonov, M. Community-level cohesion without cooperation. *Elife* **5**, e15747 (2016).

[22] Posfai, A., Taillefumier, T. & Wingreen, N. S. Metabolic Trade-Offs Promote Diversity in a Model Ecosystem. *Physical Review Letters* **118**, 028103 (2017).